Since January 2020 Elsevier has created a COVID-19 resource centre with free information in English and Mandarin on the novel coronavirus COVID-19. The COVID-19 resource centre is hosted on Elsevier Connect, the company's public news and information website.

Virus Research 223 (2016) 1–9

Contents lists available at ScienceDirect

Virus Research

journal homepage: www.elsevier.com/locate/virusres

The key molecular events during *Macrobrachium rosenbergii* nodavirus (MrNV) infection and replication in Sf9 insect cells

Monsicha Somrit[a], Atthaboon Watthammawut[a], Charoonroj Chotwiwatthanakun[b], Wattana Weerachatyanukul[a,*]

[a] *Department of Anatomy, Faculty of Science, Mahidol University, Rama VI Road, Bangkok 10400, Thailand*
[b] *Nakhonsawan Campus, Mahidol University, Nakhonsawan, Thailand*

ARTICLE INFO

Article history:
Received 12 April 2016
Received in revised form 16 June 2016
Accepted 17 June 2016
Available online 18 June 2016

Keywords:
MrNV
Virus replication
Sf9
Caveolin-mediated endocytosis pathway

ABSTRACT

In this study we demonstrated that *Macrobrachium rosenbergii* nodavirus (MrNV) was able to internalize and replicate in Sf9 insect cells, with levels of infection altered by substances affecting the caveolin-(CAV) mediated endocytosis pathway. The use of Sf9 cells for efficient MrNV replication and propagation was demonstrated by confocal microscopy and PCR amplification, through which early viral binding and internalization were initially detectable at 30 min post-infection; whereas at 72 h, the distinguishable sign of late-MrNV infection was observable as the gradual accumulation of a cytopathic effect (CPE) in the cells, ultimately resulting in cellular disruption. Moreover, during the early period of infection, the MrNV signals were highly co-localized with CAV1 signals of the CAV-mediated endocytosis pathway. The use of genistein as an inhibitor of the CAV-mediated endocytosis pathway significantly reduced MrNV and CAV1 co-localization, and also reduced the levels of MrNV infection in Sf9 cells as shown by PCR and ELISA. Moreover, the addition of the pathway agonist okadaic acid not only recovered but also augmented both the levels of MrNV co-localization with CAV1 and of Sf9 infection in the presence of genistein inhibition; therefore demonstrating that MrNV infection in Sf9 cells was associated with the CAV-mediated endocytosis pathway machinery.

1. Introduction

Macrobrachium rosenbergii nodavirus (MrNV) is one of the known causative agents of white tail disease (WTD) in the giant freshwater prawn *Macrobrachium rosenbergii*. Early WTD can be observed as the appearance of a whitish coloration in the muscles of post-larvae (PL) prawns. The later stages of the disease manifests as a sudden, 100% rate of mortality of PL in the rearing ponds, resulting in extensive damage to closed-hatchery giant freshwater prawn aquaculture (Azad et al., 2005; Bonami et al., 2005). Regarding the causative virus, MrNV is a 30 nm, non-enveloped icosahedral virus containing a linear bipartite positive-sense single-stranded RNA (ssRNA+) genome. Similar to other nodaviruses, MrNV has been shown to infect a broad spectrum of cells and organisms, ranging from mosquito cell cultures (C6/36) and aquatic insects to other types of prawn such as *Penaeus monodon* and *Litopenaeus vannamei* (Hayakijkosol and Owens, 2013; Sahul Hameed et al., 2004; Sudhakaran et al., 2008; Sudhakaran et al., 2007b).

The detection of MrNV infection in susceptible organisms has been performed through conventional techniques such as polymerase chain reaction (PCR) and immuno-detection (Pillai et al., 2006; Romestand and Bonami, 2003). Nevertheless, studies into the actual process of viral entry and infection at the intracellular level have been constrained by difficulties in maintaining stable primary cell cultures of aquatic organisms (Lu et al., 1995). Furthermore, these difficulties have been compounded by the lack of reliable continuous crustacean cell lines that would otherwise permit the long-term observations required for studying MrNV infection and replication pathways. Recent studies utilizing continuous mosquito cell lines have somewhat useful in studying MrNV infection and propagation; nevertheless, the maintenance of this particular cell line for long-term culture still proved problematic. To overcome the aforementioned difficulties, we have demonstrated the susceptibility of an insect cell line, Sf9, to MrNV infection; in addition, demonstrated the use of the cell line to facilitate in-depth studies of viral infection pathway.

* Corresponding author at: Department of Anatomy, Faculty of Science, Mahidol University, Rama VI Road, Ratchathewi, Bangkok 10400, Thailand.
E-mail address: wattana.wee@mahidol.ac.th (W. Weerachatyanukul).

http://dx.doi.org/10.1016/j.virusres.2016.06.012
0168-1702/

In general, the early phase of the infection pathway of non-enveloped viruses involves the receptor-based attachment of viral particles to the targeted cell surface, followed by the internalization of the virus into the cytoplasm. The viral entry of alpha-nodaviruses, in particular the entry of the flock house virus (FHV) into *Drosophila melanogaster* culture cells, serves as a useful starting model for further insightful investigations into the mechanism of entry of other members of the nodavirus family (Odegard et al., 2010), (Walukiewicz et al., 2006). When compared to FHV, however, limited information is available regarding the early process of MrNV infection in its natural hosts or in susceptible insect cell cultures. Given the similar icosahedral structures of both viruses, it is therefore tempting to assume that MrNV follows a similar process of endosome-dependent host-cell entry as that of its nodavirus counterparts and of non-enveloped viruses that infect mammalian cells. Small ssRNA viruses such as the picornaviruses have been extensively reported to interchangeably utilize clathrin (CLA)- and caveolin (CAV)-mediated endocytosis, whereas other similar viruses such as the poliovirus have been found to not be dependent on either pathway (Brandenburg et al., 2007; Hogle, 2002). Accordingly, further in-depth studies into the process of entry and trafficking of MrNV is required. For those purposes, the selection of host cells that reliably demonstrates susceptibility to viral infection, replication, propagation as well as permit long-term viral pathway studies would therefore be crucial.

In this study, we demonstrated the ability of MrNV to internalize and replicate in the Sf9 insect cells, the former event of which appeared to favor CAV-dependent endocytosis while the latter event was evident by a distinct cytopathic effect (CPE) and a rapid increase in virus copy number in the infected Sf9 cells. Furthermore, early MrNV infection period that is believed to be associated with CAV-mediated endocytosis is proven by inhibiting or re-activating the pathway by genistein and okadaic acid, the substances that are extensively use for studying viral infection via tyrosine-phosphate dependent caveolin-internalization pathway.

2. Materials and methods

2.1. MrNV inoculum preparation

Macrobrachium rosenbergii nodavirus (MrNV) was isolated from MrNV- infected post-larvae that were identified by the whitish discoloration of their tail muscles. The MrNV inoculum was prepared as described previously (Ravi et al., 2010). Briefly, infected tissues of *M. rosenbergii* larvae were minced and homogenized in sterile phosphate-buffered saline (PBS: 137 mM NaCl, 2.7 mM KCl, 10 mM Na_2HPO_4, 2 mM KH_2PO_4). The crude sample was then centrifuged (400*g*, 4 °C, 10 min) to eliminate crude debris. The collected supernatant was further centrifuged (12,000*g*, 4 °C, 30 min) and subsequently passed through 0.22 μm filters. The inoculum obtained was then added immediately to Sf9 cultured cells in the virus infection experiments described below.

2.2. Sf9 cell culture and MrNV infection experiments

Sf9 cells were cultured with serum-free medium (SF-900 III SFM) containing 1× antibiotic-antimycotic (Gibco, Grand Ireland, NY) in 25 ml flasks at 27 °C, with the medium replaced every two days. After reaching >90% confluence, the cells were dislodged and sub-cultured on 6-well plates at a concentration of 2×10^6 cells/well and were further cultured for another day. The cells were pre-chilled at 4 °C, and the inoculum containing MrNV was added into the medium at a final concentration of 40 μg/ml followed by continuous, gentle shaking. After incubation (4 °C, 1 h), the excess MrNV inoculum solution was removed and replaced with new medium and incubated further at various time points: 30 min, 2hr and 72 h. To observe cell viability, cells were stained with trypan blue and observed with light microscopy. The other portion of cells was harvested to perform either protein/RNA extractions or indirect immunofluorescent staining (IIF).

Table 1
Primer pairs used in this study.

Gene	Primer sequence
MrNV (RNA2)	(F) 5′- CCATGGCTAGAGGTAAACAAAATTCTA-3′
	(R) 5′- CTCGAGCTAATGATGATGATGATGATG-3′
Sf9 actin	(F) 5′- AGAAGATCTGGCACCACACC-3′
	(R) 5′- GTCATCTTCTCTCTGTTGGCCTT-3′

2.3. Semi-quantitative reverse transcriptase-polymerase chain reaction (RT-PCR)

Sf9 cells were collected and homogenized in Isol-RNA lysis reagent (5-PRIME Inc., Gaithersburg, MD) following the manufacturer's protocols to obtain purified total RNA. The RNA samples were treated with RNase-free diethylpyrocarbonate (DEPC) water and subjected to RT-PCR using a Superscript III One Step RT-PCR kit (Invitrogen, Eugene, CA). The PCR amplification was run for 40 cycles as follows: preheated at 95 °C for 5 min followed by cycles of 95 °C for 60 s; 60 °C for 30 s and 72 °C for 60 s. MrNV capsid protein-specific primers (Table 1) were designed from the nucleotide sequences available in the GenBank database (accession # JQ418298). Amplification of Sf9 actin (an internal control, Table 1) was conducted in the separated PCR reaction tubes using the same PCR conditions described above. The obtaining PCR products of MrNV and actin were mixed for co-electrophoresis. The PCR bands were then visualized by ethidium bromide staining. Comparisons of RNA expression levels were performed by densitometric analyses using Image J software (Schneider et al., 2012).

2.4. Indirect immunofluorescence (IIF) and confocal microscopy

The harvested Sf9 culture cells were fixed with 4% paraformaldehyde (30 min, room temperature) and washed with PBS. Free aldehydes were quenched with 30 mM glycine in PBS and cells were then washed twice with PBS containing 0.2% Tween 20 (PBS-T). Non-specific antibody staining was blocked with 4% bovine serum albumin (BSA) and the cells were exposed to 1:500 mouse anti-MrNV antibody in blocking solution (0.5% BSA in PBS-T). This monoclonal antibody (a kind gift from Prof. Paisan Sithigorngul, Srinakarinwirot University, Thailand) has been shown to possess high specificity towards the MrNV capsid protein (Longyant et al., 2012; Wangman et al., 2012). The cells were also exposed to monoclonal antibodies against caveolin-1 (CAV1) and the clathrin (CLA) heavy chain (Santa Cruz Biotechnology Inc., Dallas, TX) at a concentration of 1–2 μg/ml. Thereafter, cells were further incubated with goat anti-mouse Alexa 594 or Alexa 488 (Invitrogen, Carlsbad, CA) at a dilution of 1:1000 and were counterstained with either DiI (1,1′-Dioctadecyl-3,3,3′,3′-tetramethylindocarbocyanine perchlorate (DiI; $DiIC_{18}(3)$) or Oregon Green 488-conjugated 1,2-dihexadecanoyl-sn-*glycero*-3 phosphoethanolamine (DHPE; 1:5000) for labeling membrane-bound organelles, and with 4′,6-diamidino-2-phenylindole dihydrochloride (DAPI) for nuclear staining.

For confocal microscopy, the cells were plated on glass slides and topped with coverslips, and the images were acquired by an Olympus FV1000 confocal microscope. The samples were excited by argon and krypton laser lines and the fluorescent emissions were screened by 520 nm and 590 nm band-pass filters. A line-by-line

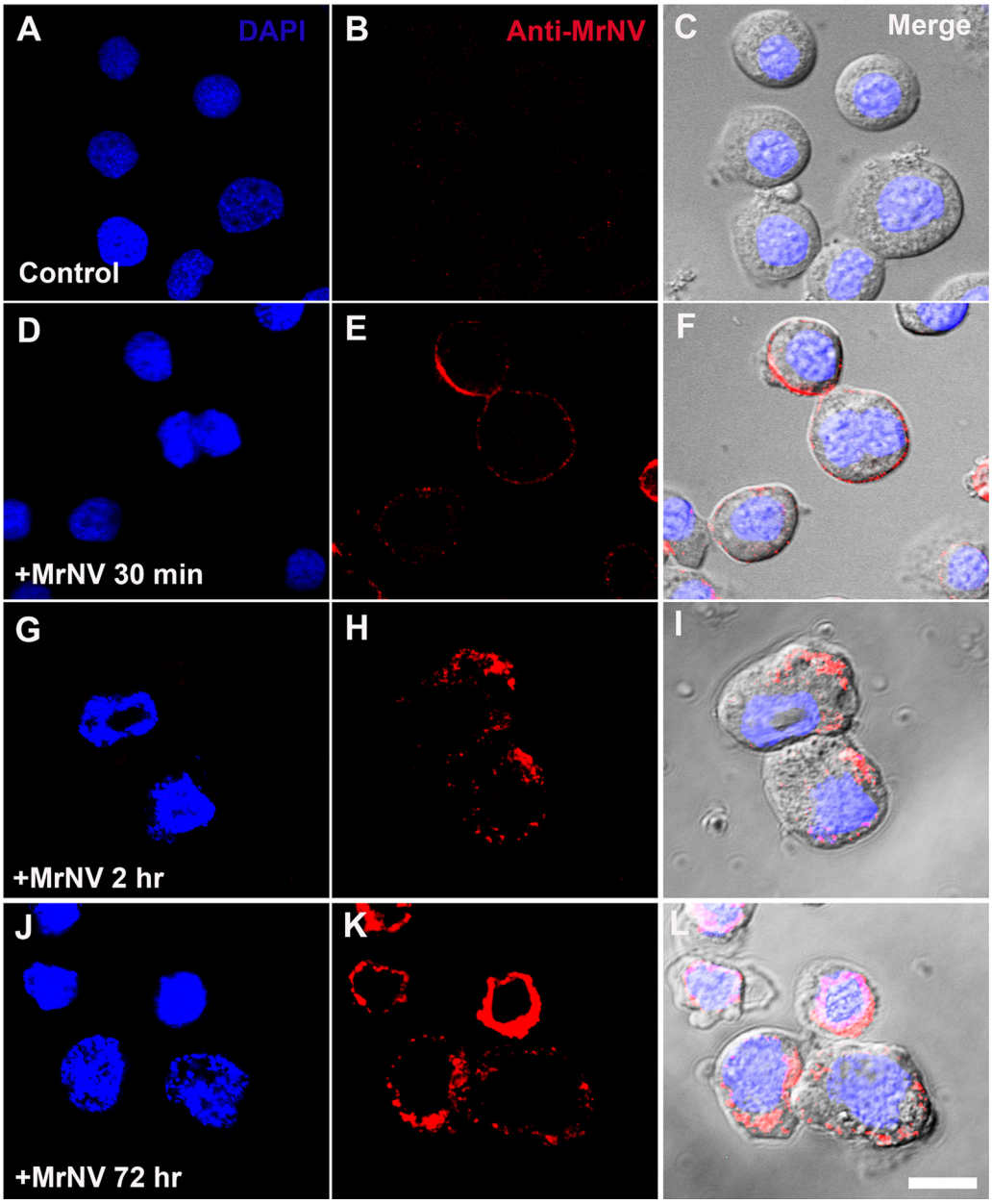

Fig. 1. Time-course confocal microscopy of MrNV infection in Sf9 cells. MrNV inoculum was introduced into cultured Sf9 cells at 4 °C, and the progress of infection was observed at 30 min, 2 h, and 72 h. The particles of MrNV were localized using anti-MrNV followed by Alexa 594-conjugated secondary antibody (red). The nuclei were counterstained with DAPI (blue). Panels C, F, I and L are the merged fluorescent micrographs with their corresponding DIC images. Bar = 10 μm. (For interpretation of the references to colour in this figure legend, the reader is referred to the web version of this article.)

with Kalman scanning mode was also applied to minimize cross-interaction of emission beams.

2.5. Pre-embedding staining and transmission electron microscopy (TEM)

Non-infected and MrNV-infected Sf9 culture cells were stained in the suspension with monoclonal anti-MrNV antibodies by the protocol described above. After washing, the cells were exposed to protein A-conjugated with 10 nm colloidal gold (Electron Microscopy Sciences, Hatfield, PA). The cells were further incubated with 1% tannic acid for 1 h to enhance visualization under a TEM. They were then dehydrated with increasing percentages of ethanol, infiltrated with a mixture of dioxane and ethanol and finally embedded in an Epon resin (Electron Microscopy Sciences, Hatfield, PA). Thin sections 70 nm thick were cut, post-stained with 1% uranyl acetate for contrast development and visualized under a Tecnai 20 FEI microscope operated at 80 kV.

2.6. Treatment of MrNV-infected Sf9 cells with either inhibitor or agonist of the CAV-mediated endocytosis pathway

Because the level of caveolin-1 expression was altered during MrNV infection (see Fig. 2 for details), we investigated the inhibition of MrNV entry through treatment of Sf9 cells by the general CAV-mediated endocytosis pathway inhibitor genistein. Sf9 cells were separated into four experimental groups: cells that were (1) maintained in SF-900 III SFM culture medium i.e. control cells; (2) incubated with MrNV inoculum on ice for 1 h in culture medium; (3) pretreated with 200 μM genistein for 30 min before

incubation with MrNV inoculum; (4) pretreated with 200 μM genistein for 30 min before co-incubation with the 30 nM okadaic acid (CAV1 agonist) + MrNV inoculum 30 min–2 h; (5) treated with 30 nM okadaic and MrNV inoculum; and (6) treated with 40 μM chlorpromazine (CLA inhibitor) or 50 μg/ml transferrin (CLA agonist) for 30 min followed by addition of MrNV inoculum. After washing with PBS, cells were then harvested either for RNA extraction (and subsequent PCR amplification), IIF or ELISA experiments as described below.

2.7. Enzyme-linked immunosorbent assay (ELISA)

Approximately 100 μg/ml of Sf9 extracted proteins (as measured by bicinchoninic acid protein assay or BCA) from four different experimental groups (control, MrNV-infected CAV-mediated pathway-inhibited and CAV-mediated pathway-reactivated groups) were diluted in coating buffer (0.1 M Na_2CO_3, 0.1 M $NaHCO_3$, pH 9.5), and the samples coated on 96-well microtiter plates overnight at 4 °C. Excess proteins were washed out with PBS-T and the coated proteins were incubated with 4% BSA (2 h, room temperature). The wells were then incubated with anti-MrNV monoclonal antibodies (1:500), followed by incubation with their corresponding secondary antibodies (1:3000) conjugated with horseradish peroxidase (HRP). To visualize protein-antibody complexes, each well was incubated with a SureBlue™ TMB peroxidase substrate (KPL, Gaithersburg, MA). After extensive washing with PBS, the intensity of the developed enzymatic products was detected with a spectrophotometer at 450 nm wavelength. Comparison of ELISA and PCR data were performed by a *t*-test statistical analysis. *P*-value of <0.01 was considered statistical difference.

3. Results

3.1. Time course of MrNV infection and replication in sf9 cells

MrNV is known to infect a broad spectrum of aquatic organisms ranging from fish to crustaceans (Hayakijkosol and Owens, 2013; Sahul Hameed et al., 2004; Sudhakaran et al., 2008, 2007b, 2006). Here, we added the list of MrNV infectivity in the cultured Sf9 insect cells. Time course studies upon addition of MrNV inoculum to Sf9 cells revealed that MrNV particles were detected on the surface of Sf9 cells as early as 30 min p.i. and then internalized and accumulated within the submembranous vicinity at 2 h p.i. The particles eventually spread throughout the cytoplasm including the supranuclear region at 72 h p.i (Fig. 1).

3.2. Co-localization of MrNV with endocytotic machinery during its internalization

We further investigated whether MrNV internalization and infection was associated with either CAV- or CLA- mediated endocytosis machinery using antibodies against MrNV- (red fluorescence – Alexa 594), and CAV1 or CLA heavy chain (green–Alexa 488). At 2 h p.i., the red fluorescent signals of anti-MrNV were highly concentrated in the peripheral cytoplasm of the infected Sf9 cells in varying patterns of distribution and degrees of intensity (Fig. 2F and N, red). Interestingly, the levels of anti-CAV1 was initially low in the non-infected cells (Fig. 2A), but were drastically increased in the 2-h MrNV-infected cells (Fig. 2E). Particularly, staining signals of anti-CAV1 were mostly co-localized with anti-MrNV signals in the submembranous areas of the cells (demonstrated by the overlapping of green and red fluorescent signals to become yellowish-orange signals) (Fig. 2H). The staining of anti-CLA which was also at the low level in the non-infected cells (Fig. 2I) remained unchanged and minimally colocalized with anti-MrNV in the MrNV infected cells (Fig. 2P). These results suggested that MrNV infection caused an enhanced expression of CAV1 (but not CLA) in MrNV-infected Sf9 cells, which were microscopically evident to be co-localized with MrNV in the submembranous vicinity.

3.3. Inhibition and resumption of MrNV internalization by genistein and okadaic acid

It has been extensively shown that caveolin-mediated endocytosis (tyrosine phosphorylation dependent) could be greatly inhibited and reactivated by genistein and okadaic acid, both of which have less disturbance on a threonine phosphorylation dependent CLA pathway) (Anderson et al., 1996; Damm et al., 2005). The levels of MrNV protein and CAV1 in the infected Sf9 cells was checked by immunofluorescence microscopy and ELISA. An apparent cease of MrNV together with CAV1 staining signals in the Sf9 cells were evident upon treating with genistein (Fig. 3I–H). Quantitative ELISA results also confirmed significant reduction of MrNV protein by 2.8-fold (Fig. 4A) upon genistein treatment. These inhibitory effects of genistein on MrNV infection were overturned when the Sf9 cells were concurrently treated with 30 nM okadaic acid, a known CAV-mediated endocytotic pathway agonist. The Sf9 cells treated with okadaic acid after genistein inhibition exhibited the higher MrNV and CAV1 staining signals (Fig. 3M–P) and its augmentation of the infection level as reflected by an ELISA results (Fig. 4A, dotted bar). It should be noted that the augmented anti-MrNV fluorescent signals was notably co-localized with anti-CAV1 staining signals in the submembranous vicinity (Fig. 3P). Sf9 cell treatment with okadaic acid alone gave a similar result as those pretreated with genistein followed by okadaic acid (data not shown). In addition, Sf9 cells treated with CLA inhibitor (chlorpromazine) or CLA agonist (transferrin) did not markedly affected MrNV infection (Supplementary Fig. S1 in the online version at DOI: 10.1016/j.virusres.2016.06.012).

We also measured the mRNA level of the infected MrNV in the Sf9 cells treated with genistein and/or okadaic acid. The levels of MrNV RNA at the band of 1.1 kbp in the PCR amplification were significantly reduced by ~2.7-fold in the genistein treated group compared with the untreated MrNV-infected cells (Fig. 4B). Recovery of MrNV infection and its augmentation by okadaic acid (Fig. 4B) well agreed with the ELISA results mentioned above. Altogether, these results suggested that the MrNV appeared to highly associate with CAV1-positive structures during the early infection period, and that the levels of internalization and infection of MrNV in Sf9 cells could be interfered with substances that either inhibited or re-activated the CAV-mediated endocytosis pathway.

3.4. Cytoplasmic changes of sf9 cells upon a prolonged MrNV infection

At the 72 h infection time point, an apparent cytopathic effect (CPE) was manifested as cytoplasmic swelling, an increased in cell size to be 20–30 μm, aggregation of cells into clumps of various sizes and extensive cellular vacuolation (Fig. 5B, arrowheads). The Sf9 cells also exhibited an apparent granularity within their cytoplasm. As revealed by confocal microscopy, positive intense red signals of anti-MrNV staining were either in a punctate pattern scattered throughout the cytoplasm or in a clustered pattern presumably in CPE at one side of the supranuclear cytoplasm within the MrNV-infected Sf9 cells (Fig. 5C–E). Non-infected cells showed a uniform spherical shape with sizes between 10 and 12 μm (Fig. 5A).

We further employed immunogold TEM localization to verify that the cytoplasmic CPE was the site/organelle where the MrNV particles were destined in the cytoplasm, not in the nucleus of the infected cells. The results revealed extensive gold deposition which

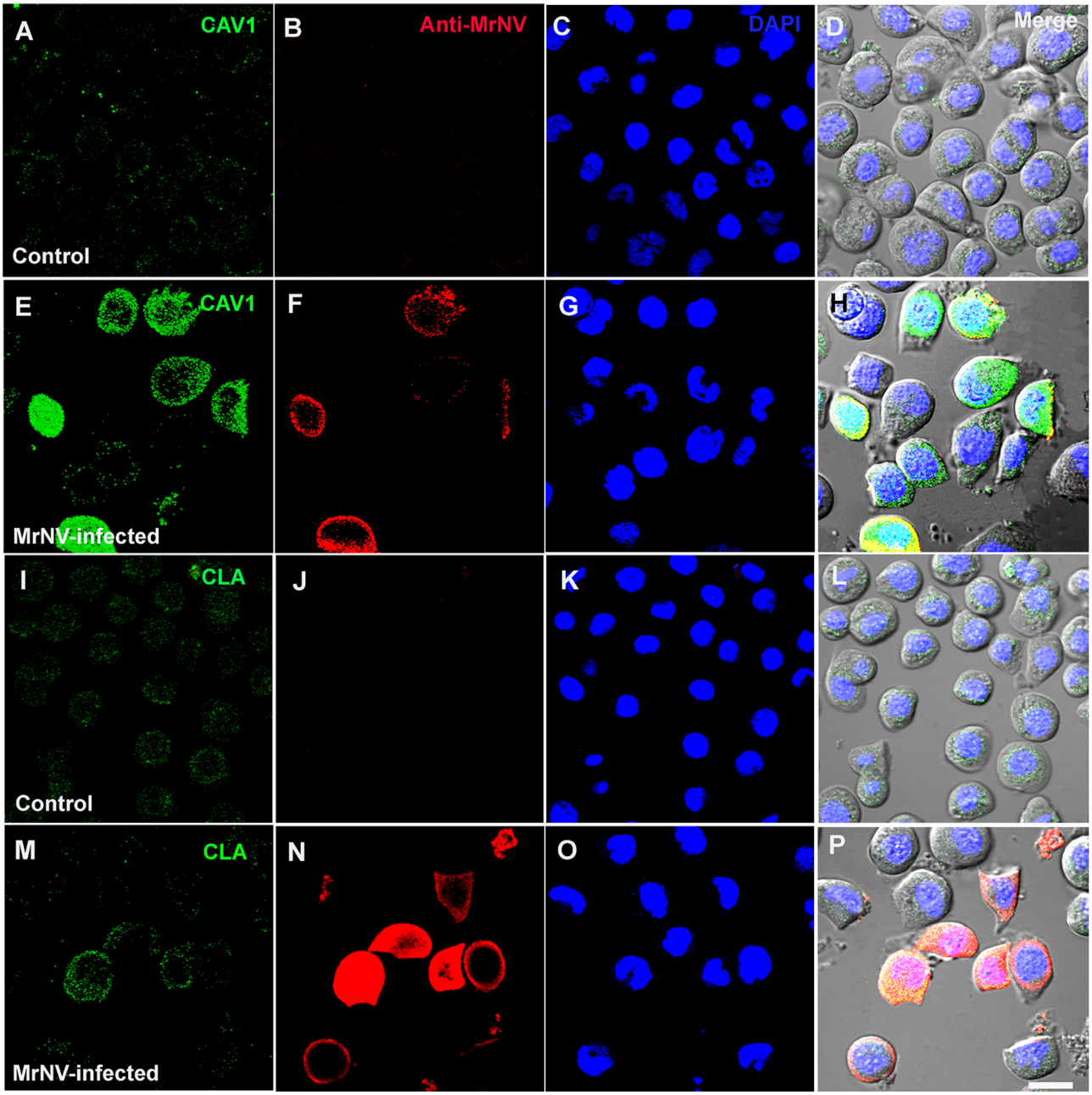

Fig. 2. Co-localization of MrNV and CAV1 in the 2 h MrNV-infected Sf9 cells. Non-infected (panels A–D and I–L) and infected Sf9 cells (panels E–H, and M–P) were probed with anti-MrNV (red, Alexa 594), anti-CAV1 or anti-CLA (green, Alexa 488) and counterstained with nuclear staining dye (blue, DAPI). Note that MrNV is mostly co-localized with CAV-1 signals in the MrNV-infected cells (panel H, yellow), but minimally co-localized with CLA signals (panel P). Bar = 10 μm. (For interpretation of the references to colour in this figure legend, the reader is referred to the web version of this article.)

was indicative of MrNV particles within the heterogeneous matrix of a large membrane-bound endosomal-like compartment (Fig. 6A and B), a typified CPE structure in the infected cells. Neither the deposition of gold particles within the cytoplasm nor the CPE feature was detected in the non-infected Sf9 cells (Fig. 5C). We thus determined that 72 h p.i. was considered the late infection stage where MrNV underwent its replication to produce extensive virions within the cytoplasm of the targeted cells.

The comparative levels of MrNV replication within the Sf9 cytoplasm was checked by immunoblotting and PCR amplification at 2 and 72 h p.i. MrNV protein immunoreactivity at 42 kDa could readily be visualized at 2 h p.i. and its band intensity was greatly enhanced at 72 h p.i. Likewise, detection of MrNV RNA could also be evident at 1.1 kbp band at the 2-h p.i. The intensity level of this band drastically increased at 72 h p.i., signifying a robust amplification of virion number within the infected cells. This relatively fast replication of this virus within Sf9 cells indicate that the cultured Sf9 insect cells are highly susceptible cells that facilitate further in-depth studies into MrNV or other nodavirus internalization and replication processes.

4. Discussion

Studies of the MrNV viral infection pathway have encountered difficulties regarding the availability of stable cell lines from aquatic animals (Jose et al., 2010). Apart from the lack of stable cell lines from naturally susceptible organisms, other complications include an isolation of potent viral inoculum; as MrNV inoculum has to be

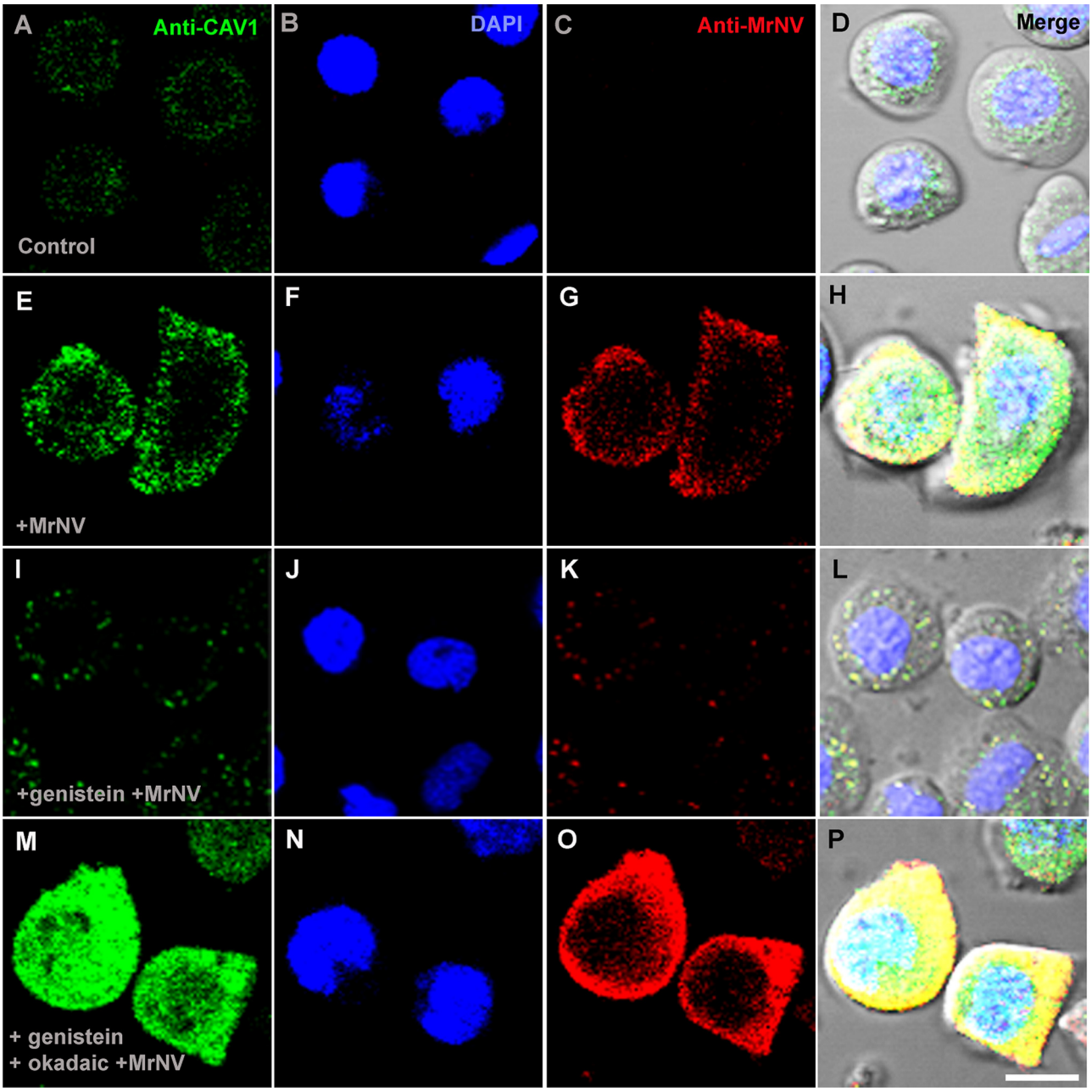

Fig. 3. Inhibition and reactivation of MrNV and CAV1 reactivity in the infected Sf9 cells. Note the corresponding increase and co-localization of MrNV protein and CAV1 in the 2 h MrNV-infected Sf9 cells (panels E–H) as compared to non-infected Sf9 cells (panels A–D). Reduction in the fluorescent signals of MrNV and CAV1 thus their co-localization is observed upon pretreating the cells with genistein (panels I–L). Sf9 cells treated with genistein followed by the incubation with okadaic acid together with MrNV inoculum resumed intracellular MrNV and CAV1 fluorescent signals and their co-localization (panels M–P). Bars = 10 μm.

obtained from post-larva prawn through the identification of the white discoloration in the infected muscle tissues (Bonami et al., 2005; Owens et al., 2009; Wang et al., 2008). This difficulty is due to the fact that infected adult animals are sometimes asymptomatic and capable of viral clearance in varying degrees (Ravi et al., 2010). In addition, an isolated MrNV inoculum is sometimes contaminated with other pathogens that do not contribute to the occurrence or progression of WTD (Qian et al., 2003; Sahul Hameed et al., 2004; Sudhakaran et al., 2007a; Zhang et al., 2006). In regard to culture systems for MrNV infection-susceptible cells and tissues; primary cultures of hemocytes or hematopoietic tissues in crustaceans have been established for the observation of viral infection (Jie Du et al., 2012). However, isolated hemocytes and hematopoietic tissues of crustaceans have to been shown to be limited in long-term stability, and hence do not facilitate extended observations of viral infection. Furthermore, other cell culture systems have exhibited varying degrees of susceptibility or permissivity to MrNV. In fact, some cell cultures such as C6/36, while susceptible to MrNV infection, are deemed to be non-permissive or unable to allow the virus particles to propagate over time, while those that allow for limited propagation are described as semi-permissive (Hayakijkosol and Owens, 2013). To circumvent the problem of unstable infected-tissue cultures, we successfully utilized the continuous Sf9 insect cell line for MrNV replication and propagation, which further allowed us to investigate MrNV infection and subsequent internalization events.

After 72-h exposure to live MrNV inoculum, the Sf9 cells exhibited characteristic signs of CPEs that included vacuolation, swelling, syncytia, aggregation and subsequent cell death (Fig. 5). These signs

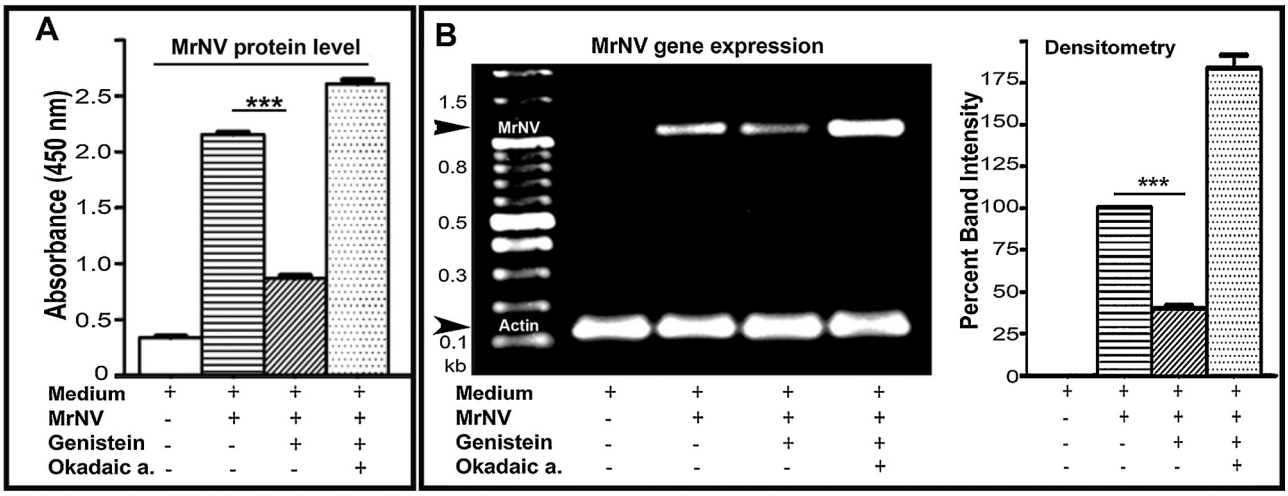

Fig. 4. Quantitative analyses of MrNV proteins and RNA expressions in various conditions of MrNV infection. ELISA analysis indicated that MrNV protein expression could be inhibited by genistein, but it could also be rescued by okadaic acid treatment (panel A). PCR amplification of MrNV gene in the Sf9 infected cells at 2 and 72 h p.i. and their densitometric analysis were shown in panel B. Arrowheads indicate PCR products of MrNV RNA at 1.1 kbp and actin (internal control) at 0.2 kbp. Asterisks (***) denote statistical difference at the *P*-value < 0.0001.

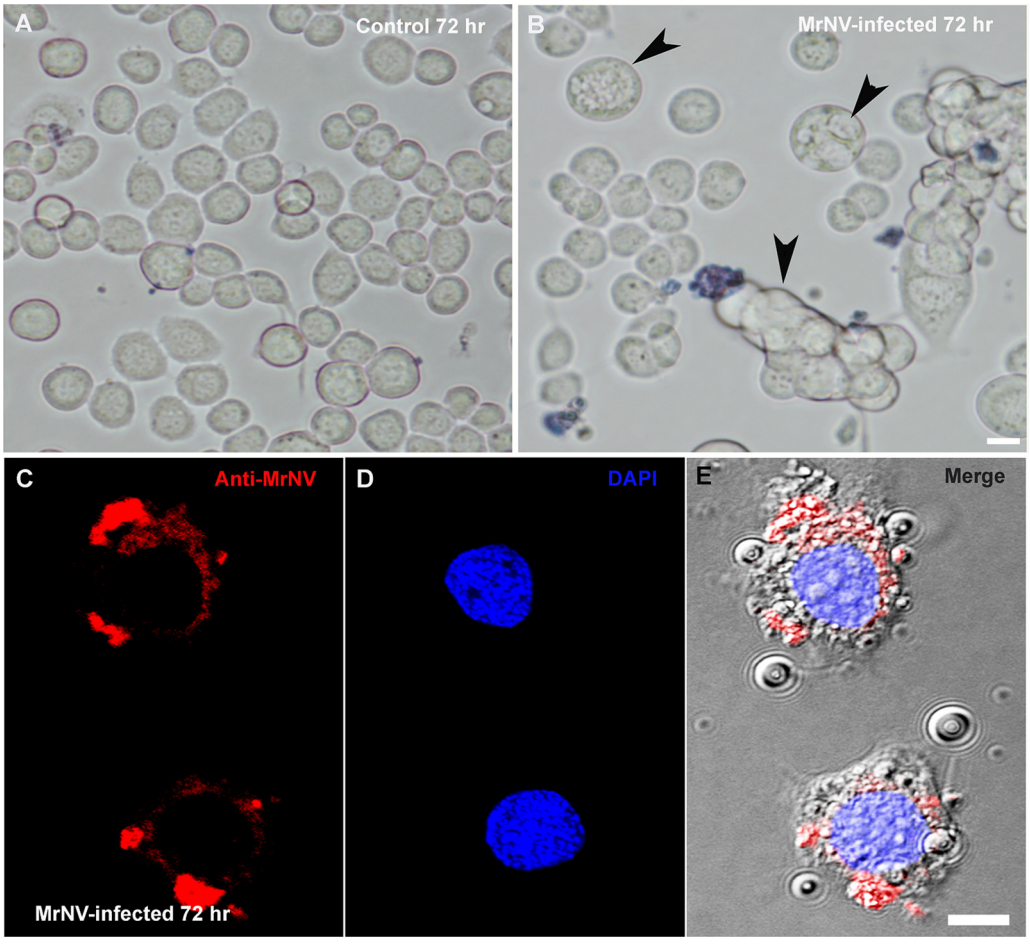

Fig. 5. MrNV-induced cytopathic effect (CPE) in the 72 h infected Sf9 cells. The uniform shape and size of the non-infected cells (panel A) were compared with the swollen, aggregated and intensely trypan blue-staining in the MrNV-infected cells (panel B). Arrowheads indicate cytopathic effects (CPE) in the cytoplasm of the swollen infected cells. Confocal microscopy of MrNV infected cells (panels C–E) were probed with anti-MrNV followed by Alexa 594-conjugated secondary antibody (red) and DAPI nuclear staining (blue). Panel E is a merged fluorescent micrograph and its corresponding DIC image. Bars = 10 μm. (For interpretation of the references to colour in this figure legend, the reader is referred to the web version of this article.)

of CPE have also been reported in MrNV-infected C3/36 mosquito cell lines (Hayakijkosol and Owens, 2013; Sudhakaran et al., 2007b), SISE embryonic sea bass cell lines and SSN-1 snakehead fish cell lines (Hernandez-Herrera et al., 2007). More importantly, we have shown by RT-PCR and ELISA that the number of virions significantly increased over an extended period (Fig. 4). Moreover, the

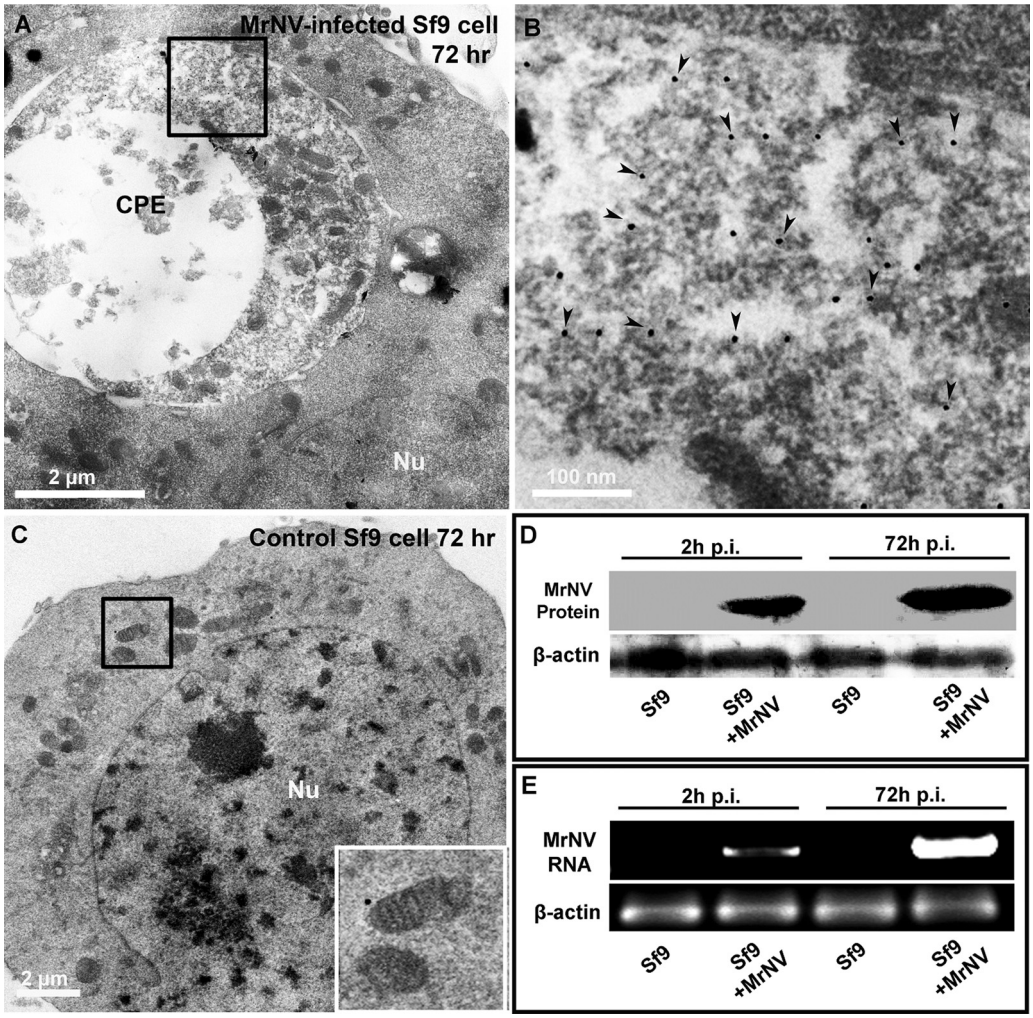

Fig. 6. Ultrastructures of 72 h MrNV-infected Sf9 cells and the comparative immunoblotting and PCR profiles of viral infection at 2 h and 72 h p.i. Deposition of gold particles (panels A and B, arrowheads) revealed the localization of MrNV particles being confined within the matrix-filled, large endosomal-like vesicles, a feature that was not present in the non-infected cells (panel C). An apparent increase of the immunoreactive 42 kDa band of MrNV protein at 72 h p.i (panel D) well corresponded with the pattern of 1.1 kbp PCR band of MrNV RNA (panel B, arrowhead).

specific replicating site of MrNV as visualized by immunogold TEM localization was confined to the membrane bound endosomal-like vesicles, signifying CPE in the infected Sf9 cells (Fig. 6). These results corroborated with similar electron microscopic findings in MrNV-infected SISE and C3/36 cell lines in which MrNV particles gathered in large, membrane-bound organelles (Hayakijkosol and Owens, 2013; Sudhakaran et al., 2007b). Our preliminary results also showed that MrNV that had replicated in Sf9 cells can be collected as inoculum to infect other Sf9 cells and prawn, suggesting the horizontal propagation ability of this virus. Nonetheless, the vertical permissiveness of the Sf9 cell culture to the virus through repeated culture passages requires further investigation.

We have provided evidence herein that favored CAV-mediated internalization during infection of MrNV. Firstly, the corresponding up-regulation between MrNV and CAV1 as well as their highly co-localized patterns under confocal microscopy at 2 h infection. Secondly, the results revealed the ability of tyrosine phosphorylation inhibitor, genistein, to virtually halt the internalization of MrNV particles, although specific inhibitors of other process within the endocytosis pathway need to be employed to provide conclusive evidence of the involvement of the CAV-mediated endocytosis pathway. Thirdly, MrNV infection could be quickly recovered and even further augmented by the pathway agonist okadaic acid (Figs. 3 and 4). Applications of genistein and okadaic acid as a potent inhibitor and agonist, respectively, of the CAV-mediated endocytotic pathway have been reported in many previous studies, in particular those pertaining to viral infections (Damm et al., 2005; Parton et al., 1994; Thomsen et al., 2002). These results correlate well with the findings in ssRNA+ viruses such as Human coronavirus 229E (Nomura et al., 2004) and Echovirus-1 (Marjomaki et al., 2002) which have been shown to be dependent on CAV-mediated endocytosis for internalization. While our results did suggest that MrNV infection in Sf9 cells were associated with the CAV-mediated endocytotic machinery, whether the viruses do internalize via caveosome-like structures at the ultra-high resolution microscopy is currently under investigation. In conclusion, we have demonstrated the effectiveness of using Sf9 insect cell line for MrNV replication and propagation, and that MrNV internalization favored more the CAV-mediated endocytostic pathway which would facilitate further detailed studies of MrNV infection/replication in this host cell line in the future.

Acknowledgments

This research was supported by grants or funding from the following: (1) Thailand Research Fund (TRF) through a Royal Golden Jubilee Ph.D. program (RGJ grant no. PHD/0171/2551), (2) Faculty of Graduate Studies, Mahidol University and (3) Faculty of Sci-

ence, Mahidol University under the National Research University Initiative (NRU). The authors would also like to thank all assistance provided by the scientists at the Central Instrument Facility (CIF), the Center of Excellence in Shrimp Biotechnology (Centex) and the Center of Nanoimaging (CNI), Faculty of Science, Mahidol University.

References

Anderson, H.A., Chen, Y., Norkin, L.C., 1996. Bound simian virus 40 translocates to caveolin-enriched membrane domains, and its entry is inhibited by drugs that selectively disrupt caveolae. Mol. Biol. Cell 7 (11), 1825–1834.

Azad, I.S., Shekhar, M.S., Thirunavukkarasu, A.R., Poornima, M., Kailasam, M., Rajan, J.J., Ali, S.A., Abraham, M., Ravichandran, P., 2005. Nodavirus infection causes mortalities in hatchery produced larvae of Lates calcarifer: first report from India. Dis. Aquat. Organ. 63 (2–3), 113–118.

Bonami, J.R., Shi, Z., Qian, D., Sri Widada, J., 2005. White tail disease of the giant freshwater prawn, Macrobrachium rosenbergii: separation of the associated virions and characterization of MrNV as a new type of nodavirus. J. Fish Dis. 28 (1), 23–31.

Brandenburg, B., Lee, L.Y., Lakadamyali, M., Rust, M.J., Zhuang, X., Hogle, J.M., 2007. Imaging poliovirus entry in live cells. PLoS Biol. 5 (7), e183.

Damm, E.M., Pelkmans, L., Kartenbeck, J., Mezzacasa, A., Kurzchalia, T., Helenius, A., 2005. Clathrin- and caveolin-1-independent endocytosis: entry of simian virus 40 into cells devoid of caveolae. J. Cell Biol. 168 (3), 477–488.

Hayakijkosol, O., Owens, L., 2013. Non-permissive C6/36 cell culture for the Australian isolate of Macrobrachium rosenbergii nodavirus. J. Fish Dis. 36 (4), 401–409.

Hernandez-Herrera, R.I., Chappe-Bonnichon, V., Roch, P., Sri Widada, J., Bonami, J.R., 2007. Partial susceptibility of the SSN-1 fish cell line to a crustacean virus: a defective replication study. J. Fish Dis. 30 (11), 673–679.

Hogle, J.M., 2002. Poliovirus cell entry: common structural themes in viral cell entry pathways. Annu. Rev. Microbiol. 56, 677–702.

Jie Du, J.O., Li, Wenjie, Ding, Zhengfeng, Wu, Ting, Meng, Qingguo, Gu, Wei, Wang, Wen, 2012. Primary hemocyte culture of the freshwater prawn Macrobrachium rosenbergii and its susceptibility to the novel pathogen spiroplasma strain MR-1008. Aquaculture 330–333, 21–28.

Jose, S., Mohandas, A., Philip, R., Bright Singh, I.S., 2010. Primary hemocyte culture of Penaeus monodon as an in vitro model for white spot syndrome virus titration, viral and immune related gene expression and cytotoxicity assays. J. Invertebr. Pathol. 105 (3), 312–321.

Longyant, S., Senapin, S., Sanont, S., Wangman, P., Chaivisuthangkura, P., Rukpratanporn, S., Sithigorngul, P., 2012. Monoclonal antibodies against extra small virus show that it co-localizes with Macrobrachium rosenbergii nodavirus. Dis. Aquat. Organ. 99 (3), 197–205.

Lu, Y., Tapay, L.M., Loh, P.C., Brock, J.A., Gose, R., 1995. Development of a quantal assay in primary shrimp cell culture for yellow head baculovirus (YBV) of penaeid shrimp. J. Virol. Methods 52 (1–2), 231–236.

Marjomaki, V., Pietiainen, V., Matilainen, H., Upla, P., Ivaska, J., Nissinen, L., Reunanen, H., Huttunen, P., Hyypia, T., Heino, J., 2002. Internalization of echovirus 1 in caveolae. J. Virol. 76 (4), 1856–1865.

Nomura, R., Kiyota, A., Suzaki, E., Kataoka, K., Ohe, Y., Miyamoto, K., Senda, T., Fujimoto, T., 2004. Human coronavirus 229E binds to CD13 in rafts and enters the cell through caveolae. J. Virol. 78 (16), 8701–8708.

Odegard, A., Banerjee, M., Johnson, J.E., 2010. Flock house virus: a model system for understanding non-enveloped virus entry and membrane penetration. Curr. Top. Microbiol. Immunol. 343, 1–22.

Owens, L., La Fauce, K., Juntunen, K., Hayakijkosol, O., Zeng, C., 2009. Macrobrachium rosenbergii nodavirus disease (white tail disease) in Australia. Dis. Aquat. Organ. 85 (3), 175–180.

Parton, R.G., Joggerst, B., Simons, K., 1994. Regulated internalization of caveolae. J. Cell Biol. 127 (5), 1199–1215.

Pillai, D., Bonami, J.R., Sri Widada, J., 2006. Rapid detection of Macrobrachium rosenbergii nodavirus (MrNV) and extra small virus (XSV), the pathogenic agents of white tail disease of Macrobrachium rosenbergii (De Man), by loop-mediated isothermal amplification. J. Fish Dis. 29 (5), 275–283.

Qian, D., Shi, Z., Zhang, S., Cao, Z., Liu, W., Li, L., Xie, Y., Cambournac, I., Bonami, J.R., 2003. Extra small virus-like particles (XSV) and nodavirus associated with whitish muscle disease in the giant freshwater prawn, Macrobrachium rosenbergii. J. Fish Dis. 26 (9), 521–527.

Ravi, M., Nazeer Basha, A., Taju, G., Ram Kumar, R., Sahul Hameed, A.S., 2010. Clearance of Macrobrachium rosenbergii nodavirus (MrNV) and extra small virus (XSV) and immunological changes in experimentally injected Macrobrachium rosenbergii. Fish Shellfish Immunol. 28 (3), 428–433.

Romestand, B., Bonami, J.R., 2003. A sandwich enzyme linked immunosorbent assay (S-ELISA) for detection of MrNV in the giant freshwater prawn, Macrobrachium rosenbergii (de Man). J. Fish Dis. 26 (2), 71–75.

Sahul Hameed, A.S., Yoganandhan, K., Sri Widada, J., Bonami, J.R., 2004. Experimental transmission and tissue tropism of Macrobrachium rosenbergii nodavirus (MrNV) and its associated extra small virus (XSV). Dis. Aquat. Organ. 62 (3), 191–196.

Schneider, C.A., Rasband, W.S., Eliceiri, K.W., 2012. NIH Image to ImageJ: 25 years of image analysis. Nat. Methods 9 (7), 671–675.

Sudhakaran, R., Yoganandhan, K., Ahmed, V.P., Hameed, A.S., 2006. Artemia as a possible vector for Macrobrachium rosenbergii nodavirus (MrNV) and extra small virus transmission (XSV) to Macrobrachium rosenbergii post-larvae. Dis. Aquat. Organ. 70 (1–2), 161–166.

Sudhakaran, R., Ishaq Ahmed, V.P., Haribabu, P., Mukherjee, S.C., Sri Widada, J., Bonami, J.R., Sahul Hameed, A.S., 2007a. Experimental vertical transmission of Macrobrachium rosenbergii nodavirus (MrNV) and extra small virus (XSV) from brooders to progeny in Macrobrachium rosenbergii and Artemia. J. Fish Dis. 30 (1), 27–35.

Sudhakaran, R., Parameswaran, V., Sahul Hameed, A.S., 2007b. In vitro replication of Macrobrachium rosenbergii nodavirus and extra small virus in C6/36 mosquito cell line. J. Virol. Methods 146 (1–2), 112–118.

Sudhakaran, R., Haribabu, P., Kumar, S.R., Sarathi, M., Ahmed, V.P., Babu, V.S., Venkatesan, C., Hameedl, A.S., 2008. Natural aquatic insect carriers of Macrobrachium rosenbergii nodavirus (MrNV) and extra small virus (XSV). Dis. Aquat. Organ. 79 (2), 141–145.

Thomsen, P., Roepstorff, K., Stahlhut, M., van Deurs, B., 2002. Caveolae are highly immobile plasma membrane microdomains, which are not involved in constitutive endocytic trafficking. Mol. Biol. Cell 13 (1), 238–250.

Walukiewicz, H.E., Johnson, J.E., Schneemann, A., 2006. Morphological changes in the T = 3 capsid of Flock House virus during cell entry. J. Virol. 80 (2), 615–622.

Wang, C.S., Chang, J.S., Wen, C.M., Shih, H.H., Chen, S.N., 2008. Macrobrachium rosenbergii nodavirus infection in M. rosenbergii (de Man) with white tail disease cultured in Taiwan. J. Fish Dis. 31 (6), 415–422.

Wangman, P., Senapin, S., Chaivisuthangkura, P., Longyant, S., Rukpratanporn, S., Sithigorngul, P., 2012. Production of monoclonal antibodies specific to Macrobrachium rosenbergii nodavirus using recombinant capsid protein. Dis. Aquat. Organ. 98 (2), 121–131.

Zhang, H., Wang, J., Yuan, J., Li, L., Zhang, J., Bonami, J.R., Shi, Z., 2006. Quantitative relationship of two viruses (MrNV and XSV) in white-tail disease of Macrobrachium rosenbergii. Dis. Aquat. Organ. 71 (1), 11–17.